Combined density functional theory and Landauer approach for hole transfer in DNA along classical molecular dynamics trajectories

P. Benjamin Woiczikowski,[1] Tomáš Kubař,[1] Rafael Gutiérrez,[2] Rodrigo A. Caetano,[2,3] Gianaurelio Cuniberti,[2] and Marcus Elstner[1,a)]

[1]*Department of Physical and Theoretical Chemistry, Technische Universität Braunschweig, D-38106 Braunschweig, Germany*

[2]*Max Bergmann Center of Biomaterials and Institute for Materials Science, Dresden University of Technology, D-01062 Dresden, Germany*

[3]*Instituto de Fisica, Universidade Federal de Alagoas, Maceio, AL 57072-970, Brazil*

(Received 27 February 2009; accepted 8 May 2009; published online 4 June 2009)

We investigate in detail the charge transport characteristics of DNA wires with various sequences and lengths in the presence of solvent. Our approach combines large-scale quantum/classical molecular dynamics (MD) simulations with transport calculations based on Landauer theory. The quantum mechanical transmission function of the wire is calculated along MD trajectories and thus encodes the influence of dynamical disorder arising from the environment (water, backbone, counterions) and from the internal base dynamics. We show that the correlated fluctuations of the base pair dynamics are crucial in determining the transport properties of the wire and that the effect of fluctuations can be quite different for sequences with low and high static disorders (differences in base ionization potentials). As a result, in structures with high static disorder as is the case of the studied Dickerson dodecamer, the weight of high-transmissive structures increases due to dynamical fluctuations and so does the calculated average transmission. Our analysis further supports the basic intuition of charge-transfer active conformations as proposed by Barton *et al.* [J. Am. Chem. Soc. **126**, 11471 (2004)]. However, not DNA conformations with good stacking contacts leading to large interbase hopping values are necessarily the most important, but rather those where the average fluctuation of ionization potentials along the base stack is small. The reason behind this is that the ensemble of conformations leads to average electronic couplings, which are large enough for sufficient transmission. On the other hand, the alignment of onsite energies is the critical parameter which gates the charge transport. © *2009 American Institute of Physics*. [DOI: 10.1063/1.3146905]

I. INTRODUCTION

DNA occupies an outstanding position in life sciences for its crucial role as the carrier of genetic code and as such, it has been the focus of intensive research during decades within the biochemistry and biophysics community. In the context of rather new field of molecular electronics,[1] DNA molecules may play a twofold role, serving either as a template by exploiting their self-assembling and self-recognition properties,[2–4] or they may be used as active wiring systems. For this latter purpose, a basic understanding of possible charge migration scenarios in such complex biomolecules is required.

The possibility of charge motion along the double helix over long distances was already demonstrated in the early 90's by the groundbreaking electron transfer experiments performed by Barton and co-workers,[5–12] Giese and co-workers,[13,14] Lewis *et al.*,[15,16] Schuster and co-workers,[17–19] and Michel-Beyerle and co-workers.[20–22] These and similar experiments revealed electron transfer occurring over distances as long as 40 Å, which was in so far surprising, as the highly disordered structure of natural DNA related to the quasirandom base pair sequence should lead to a considerable degree of charge localization. The question may then arise if charge transport through DNA may also be supported, i.e., if DNA can carry an electrical current when contacted by metallic electrodes,[23,24] and if so then under what conditions.

However, transport experiments have shown very contradictory results. Thus, DNA has been identified as an insulator,[25] a wide-band-gap semiconductor,[26] or even as a metallic conductor.[27–29] Possible reasons for this complex behavior include the following: (i) The specific base sequence of the probed molecules is essential in determining the efficiency of charge propagation, since it determines the potential profile (energy gaps) that an extra charge will "feel;" (ii) the structure of DNA (e.g., whether in A or B form) leads to a quantitative difference in the overlap of the π-electrons of the stacked bases, resulting in potentially different transport properties; (iii) the length of the sequences is of great importance: Longer chains may be deformed due to structural instability. Any kinks and defects in the DNA structure introduced in this way may distort the DNA π-system and thereby diminish the conduction significantly. As shown in the former electron transfer experiments, the transfer rates change qualitatively their length dependence going from exponential to algebraic behavior. This has been mainly explained in the frame of thermally activated incoherent hole

a)Electronic mail: m.elstner@tu-bs.de.

hopping mechanisms;[21,30–33] (iv) the DNA-metal contact topology and electronic structure are crucial; (v) dynamical effects related to the intrinsic base-pair dynamics or to the solvent fluctuations have been recognized to affect charge migration dramatically.[34–43]

As shown recently[29,44] DNA may nevertheless support large currents. Both experiments found currents of 100–150 nA at about 1 V. In Ref. 44, electrical transport through covalently Au-contacted double-stranded DNA in aqueous solution was measured, where the native form of the DNA is preserved. The *I-V* curves show a rather smooth Ohmic profile with considerably large currents up to 150 nA at 0.8 V. The experimental approach of Ref. 29 was based on measuring current through suspended double-stranded DNA molecules connected between a metal substrate and a gold nanoparticle contacted to an atomic force microscopy (AFM) conducting tip. Currents of the order of 220 nA at 2.0 V were measured. Interestingly, the length and base sequence of DNA in these two experiments were completely different.

Theoretically, the issue of charge migration through DNA has been mainly addressed on the basis of model Hamiltonian approaches,[45–57] density functional theory (DFT) calculations,[24,58–72] as well as with quantum chemical methodologies.[22,34,73–78] All these approaches possess obviously advantages and disadvantages. For instance, first-principles calculations can provide very accurate information about electronic transfer parameters, but only for static geometries, so that dynamical fluctuations cannot be taken into account in a straightforward way. Model Hamiltonians, on the other hand, offer the possibility to explore different charge transport scenarios, but they also contain many parameters that are difficult to estimate. This limits the predictive power of those models in case of complex biomolecular systems. Dynamical simulations can describe the influence of structural fluctuations but are usually based on classical approaches where the electronic structure of the biomolecule cannot be taken into account in a realistic way.

As shown previously by Voityuk and co-workers,[79–81] dynamical as well as environmental fluctuations of electronic parameters have a large impact on charge transfer in DNA. Theoretical calculations by Grozema *et al.*[82] for stilbene-linked DNA hairpins corroborate the importance of structural dynamics for hole transfer in DNA.

Recently,[42,43] we have developed a methodology which allows to include the influence of structural fluctuations and solvent effects onto the electronic structure of short DNA oligomers. Hereby we have attempted to partially overcome the difficulties inherent to the previously mentioned approaches by using a DFT-based fragment-orbital (FO) method, which allows to compute the charge transfer parameters along multinanosecond molecular dynamics (MD) trajectories. Here, solvation effects are described using a hybrid quantum mechanics/molecular mechanics (QM/MM) coupling scheme. In this way, a realistic description of both the molecular electronic structure and the conformational dynamics as well as of solvation effects can be achieved.

Our results pointed out that the fluctuation of solvent molecules can lead to large oscillations of effective onsite energies, which strongly determine the energetics of charge propagation along the DNA strand. In contrast, the interbase electronic matrix elements were found to depend only on the molecular conformation and did not seem strongly affected by the presence of solvent. Further, we showed that onsite energies are strongly correlated between neighboring nucleobases, indicating that a conformational-gating type of mechanism may be induced by the collective environmental degrees of freedom. This latter mechanism has been proposed by Barton and co-workers[83–86] in the frame of the conformational gating model. As a result, in the course of DNA dynamics, only a subset of conformations allows for efficient charge transfer; such subsets are characterized by transient domains ranging over three to five base pairs over which an electron/hole is delocalized. The charge hopping process takes place between these domains rather than between individual neighboring bases.

In this work, we will make use of our previous achievements[42,43] to investigate in more detail the transport characteristics of DNA wires with different base sequences and lengths. Our approach will combine MD simulations with transport calculations on the basis of Landauer theory. Thus, our main target will be the quantum mechanical transmission function of the wire. This quantity will be calculated along MD trajectories and will thus encode the influence of dynamical disorder arising from the environment and/or from the internal base dynamics. We will show that correlations in the base pair dynamics are crucial in determining the transport properties of the wire and that the effect of fluctuations is opposite for sequences with low and high static disorders. Hence, in homogeneous sequences like poly(G) structural fluctuations reduce the number of conformations favoring charge migration, while in structures with high static disorder as is the case of the Dickerson dodecamer, the weight of high transmissive structures increases and so does the average transmission.

In Sec. II, we describe the computational method to map the electronic structure of the DNA molecules in a solvent onto an effective low-dimensional model Hamiltonian (linear chain) as well as the transport formalism used in this paper based on Landauer's approach. In Sec. III we discuss the transport properties of several DNA chains with varying lengths and different sequences. We compare the transmission properties of static (ideal) structures with those obtained for fluctuating molecules in a solvent in Secs. III A 1–III A 3. We clearly show that the onsite energy fluctuations are giving the largest contribution in determining the charge migration efficiency. We further discuss the influence of correlated motion along the chains by comparing our results with calculations using Anderson's model of disorder in Sec. III B. Finally, a statistical analysis of the contribution of different conformations to charge transport is carried out in Sec. III C.

II. METHODOLOGY

A. Electronic structure

Before dealing with the transport problem, we will shortly describe the mapping of the full DNA electronic structure onto a general nearest-neighbor tight-binding

model, which will provide the starting point for the effective description of the biomolecule electronic properties in a solvent. The tight-binding Hamiltonian takes the form

$$H = \sum_i \epsilon_i a_i^\dagger a_i + \sum_{ij} T_{ij}^0 (a_i^\dagger a_j + \text{H.c.}), \tag{1}$$

where the onsite energies ϵ_i and the nearest-neighbor hopping integrals T_{ij}^0 characterize, respectively, effective ionization energies and electronic couplings of the molecular fragments (see below). The evaluation of these parameters can be done very efficiently using the self-consistent-charge density-functional tight-binding (SCC-DFTB) method[87] combined with a FO approach[38]

$$\epsilon_i = -\langle \phi_i | \hat{H}_{\text{KS}} | \phi_i \rangle \tag{2}$$

and

$$T_{ij}^0 = \langle \phi_i | \hat{H}_{\text{KS}} | \phi_j \rangle. \tag{3}$$

The molecular orbitals (MOs) ϕ_i and ϕ_j are the highest-occupied molecular orbitals (HOMOs) of the DNA bases i and j. Depending on the definition of FOs different tight-binding models may be designed. In our case, we use a minimal approach where the DNA electronic structure will be mapped onto a linear chain. The FOs are obtained by performing SCC-DFTB calculations of the isolated fragments, i.e., the individual Watson–Crick pairs in this case.

Applying a linear combination of atomic orbitals (LCAO) expansion

$$\phi_i = \sum_\mu c_\mu^i \eta_\mu, \tag{4}$$

the coupling and overlap integrals in the MO basis can be efficiently evaluated as

$$T_{ij}^0 = \sum_{\mu\nu} c_\mu^i c_\nu^j \langle \eta_\mu | \hat{H}_{\text{KS}} | \eta_\nu \rangle = \sum_{\mu\nu} c_\mu^i c_\nu^j H_{\mu\nu} \tag{5}$$

and

$$S_{ij} = \sum_{\mu\nu} c_\mu^i c_\nu^j \langle \eta_\mu | \eta_\nu \rangle = \sum_{\mu\nu} c_\mu^i c_\nu^j S_{\mu\nu}. \tag{6}$$

$H_{\mu\nu}$ and $S_{\mu\nu}$ are the Hamilton and overlap matrices in the atomic basis set as evaluated with the SCC-DFTB method. For additional details see Ref. 42.

The effect of environment, i.e., the electrostatic field of the DNA backbone, the water molecules, and the counterions is taken into account through the following QM/MM Hamiltonian:

$$H_{\mu\nu} = H_{\mu\nu}^0 + \frac{1}{2} S_{\mu\nu}^{\alpha\beta} \sum_\delta \Delta q_\delta (\gamma_{\alpha\delta} + \gamma_{\beta\delta}) + \sum_A Q_A \left(\frac{1}{r_{A\alpha}} + \frac{1}{r_{A\beta}} \right). \tag{7}$$

Δq_δ are the Mulliken charges in the QM region and Q_A are the charges in the MM region, i.e., the DNA backbone, counterions, and water molecules. The coupling to the environment is therefore explicitly described via the interactions with the Q_A charges. In the following, we will denote the calculation setup based on the complete expression in Eq. (7) as QM/MM; however, neglecting the last term will be denoted as "vacuo." The matrix T_{ij}^0 is built from nonorthogonal orbitals ϕ_i and ϕ_j. For many problems, a representation in an orthogonal basis set is more suitable and this can be achieved by using the Loewdin transformation[88]

$$\mathbf{T} = \mathbf{S}^{-1/2} \mathbf{T}^0 \mathbf{S}^{-1/2}. \tag{8}$$

T_{ij} can be identified with charge-transfer integrals computed, e.g., using Hartree-Fock Koopmans' theorem approximation (HF-KTA).[89] The calculation of charge transfer parameters in this way enables an extremely fast and efficient evaluation along MD trajectories, also completely including the effect of the environment using the QM/MM formalism.[42,43]

B. Charge transport through a linear chain

Once an effective model Hamiltonian for the electronic structure of DNA oligomers in a solvent has been set up, we can extend it to include the coupling to the left (L) and right (R) electrodes in order to deal with the charge transport problem

$$H = \sum_i \epsilon_i a_i^\dagger a_i + \sum_i T_{i,i+1} (a_i^\dagger a_{i+1} + \text{H.c.}) + \sum_{\mathbf{k}\in L} t_{\mathbf{k},L} (c_\mathbf{k}^\dagger a_1 + \text{H.c.}) + \sum_{\mathbf{k}\in R} t_{\mathbf{k},R} (c_\mathbf{k}^\dagger a_N + \text{H.c.}) + \sum_{\mathbf{k}\in L,R} \epsilon_\mathbf{k} c_\mathbf{k}^\dagger c_\mathbf{k}. \tag{9}$$

In the previous expression we have already taken into account that the model is a linear chain, where only sites 1 and N couple to L and R electrodes, respectively. Note also that we are using the hopping $T_{i,i+1}$ rather than $T_{i,i+1}^0$. This model Hamiltonian is a standard in quantum transport calculations.[90,91] Within the Landauer approach, the transmission function $T(E)$ for a given set of electronic parameters is immediately obtained as

$$T(E) = 4\gamma_\text{L}\gamma_\text{R} |G_{1N}(E)|^2, \tag{10}$$

where γ_L and γ_R are effective coupling terms to the L and R electrodes, respectively. Hereby we are using the wide-band approximation, replacing the energy dependent coupling terms by constants. $G_{1N}(E)$ is the 1 N-matrix element of the chain Green's function, which can be calculated via the matrix Dyson equation

$$\mathbf{G}^{-1}(E) = E1 - \mathbf{H} - \mathbf{\Sigma}_\text{L} - \mathbf{\Sigma}_\text{R},$$

$$(\mathbf{\Sigma}_\text{L})_{lj} = -i\gamma_\text{L}\delta_{l1}\delta_{j1}, \tag{11}$$

$$(\mathbf{\Sigma}_\text{R})_{lj} = -i\gamma_\text{R}\delta_{lN}\delta_{jN}.$$

Using the former expressions, the conformational (time) dependent electrical current will be simply calculated by

$$I(V) = 4\frac{2e}{h}\gamma_L\gamma_R\int dE\left(f\left(E - E_F - \frac{eV}{2}\right) - f\left(E - E_F + \frac{eV}{2}\right)\right)|G_{1N}(E)|^2. \quad (12)$$

We remark that our goal is to highlight the influence of dynamics and environment on the charge transport. Hence, we will mainly analyze time-averaged transport quantities, where the averaging is performed over MD. The conformational dynamics as well as the solvent fluctuations are encoded in these time series. At this level of theory, we are not aiming at the formulation of a microscopic transport model which would treat nonadiabatic effects. Rather, we rely on a coherent transport model with very short time scales of the order of femtosecond. This approximation should hold if the typical electronic time scales are much shorter than the period of DNA conformational dynamics.

C. Molecular dynamics approach

To study the effect of DNA conformational dynamics as well as the fluctuations of environment on the transport properties of DNA oligomers, we performed classical MD simulations in the nanosecond regime using the AMBER-parm99 force field[92] with the parmBSC0 extension[93] as implemented in the GROMACS (Ref. 94) software package. The static ideal A- and B-DNA structures were built with the 3DNA program[95] while the starting structures for the MD simulations were created using the make-na server.[96] We simulated undecamers of six regular sequences: poly(G), poly(A), poly(AT), poly(GA), poly(GC), and poly(GT), as well as the Dickerson dodecamer (base sequence: 5′-CGCGAATTCGCG-3′).[97]

After a standard heating procedure followed by a 1 ns equilibration phase, which is discarded afterward, we performed 30 ns MD simulations with a time step of 2 fs. The simulations were carried out in a rectangular box with periodic boundary conditions and filled with around 5500 TIP3P (Ref. 98) water molecules and 20 (respectively 22 for the Dickerson DNA) sodium counterions for neutralization. Snapshots of the molecular structures were saved every 1 ps, for which the charge transfer parameters were calculated with the SCC-DFTB-FO approach as described above. To assess the effect of environment, we compute these parameters with and without the external charges in Eq. (7). These external charges render the electrostatic field induced by the DNA backbone, the solvent, and the sodium counterions, see also Fig. 1. For every set of charge transfer (CT) parameters, i.e., at each time step t, we calculated the energy dependent transmission function $T(E,t)$. Here, the energy E covers the spectral support of the function and it roughly corresponds to the possible charge injection energies. We further performed the same simulations for longer DNA chains of poly(A) and poly(G) with up to 31 base pairs in order to investigate the length dependence of the transport through DNA. To focus on the fluctuations of transport properties in time we performed a shorter 100 ps MD simulation of a poly(G) undecamer with a time step of 1 fs. Here, snapshots were recorded every femtosecond.

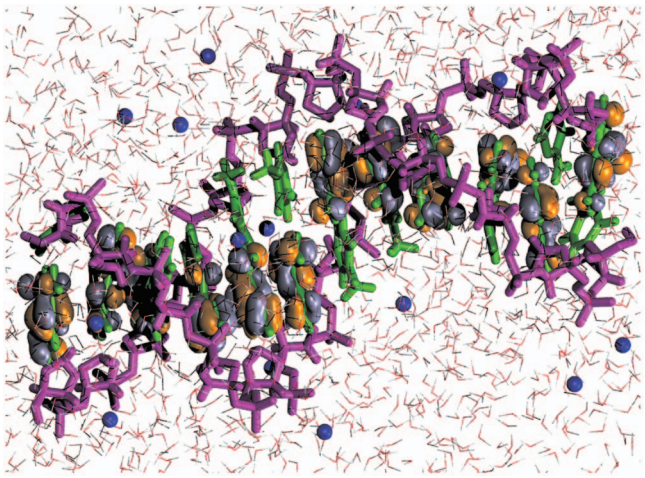

FIG. 1. (Color) MD snapshot of the Dickerson dodecamer DNA: Backbone (pink), base pairs (green), solvent molecules (red and white lines), and sodium counterions (blue spheres). Also shown are the corresponding HOMOs on each of the base pairs being almost completely localized on the purine bases. DNA backbone, solvent, and sodium counterions comprise the electrostatic environment which is described via QM/MM coupling.

III. RESULTS

In this section, we will analyze the factors governing the DNA transport properties in detail using the CT parameters evaluated along all-atom MD simulations and relying on the methodologies described in the previous paragraph. In the first paragraph, we discuss the effect of DNA internal dynamics and of environmental fluctuations. In the second paragraph, we will show that the occurring fluctuations cannot be considered to be completely random. The coherent motion of DNA bases and, in particular that of the surrounding water, turns out to be of crucial importance. Finally, the DNA conformations which are active for charge transport are addressed in more detail.

A. The influence of internal dynamics and environmental fluctuations on the transmission function

1. Transport through idealized static B-DNA

To have an appropriate reference point to estimate the influence of dynamics, the CT parameters are first calculated for ideal A- and B-DNA forms of all the previously listed sequences containing seven Watson–Crick base pairs. These static conformations are characterized by six helical parameters: rise, twist, slide, roll, shift, and tilt. Those parameters are taken as 3.2 Å, 32°, −1.5 Å, 12°, 0 Å, and 0° for A-DNA and 3.38 Å, 36°, 0 Å, 0°, 0 Å, and 0° for B-DNA, respectively.[99,100] To calculate the electronic parameters ϵ_i and T_{ij} we consider only the stacked base pairs without any environment, i.e., the term containing Q_A in Eq. (7) is omitted. Small variations occur due to small differences in the base geometries along the DNA chain. The diagonal elements of the Hamiltonian matrix ϵ_i are nearly constant within these idealized heptamers and they take values of −4.53 eV for G-C and −5.21 eV for the A-T base pairs, respectively. The electronic couplings T_{ij}, which are largely determined by the relative orientation of neighboring bases, are shown in

TABLE I. Electronic couplings T_{ij} for a hole transfer in idealized static A- and B-DNA without QM/MM environment compared to MD averaged values with standard deviations $\langle T_{ij}\rangle \pm \sigma$ including the QM/MM environment for helical parameters of the idealized A- and B-DNA. See Refs. 99 and 100. All values are in eV.

	Static B-DNA		Average MD values		Static A-DNA	
XY	5′-*XY*-3′ T_{ij}	5′-*YX*-3′ T_{ij}	5′-*YX*-3′ $\langle T_{ij}\rangle \pm \sigma$	5′-*XY*-3′ $\langle T_{ij}\rangle \pm \sigma$	5′-*XY*-3′ T_{ij}	5′-*YX*-3′ T_{ij}
Intrastrand						
AA	0.013		0.058 ± 0.037		0.070	
GG	0.052		0.029 ± 0.023		0.012	
GA	0.053	0.026	0.034 ± 0.027	0.033 ± 0.028	0.023	0.044
Interstrand						
GC	0.017	0.029	0.012 ± 0.012	0.022 ± 0.016	0.006	0.054
AT	0.035	0.031	0.037 ± 0.029	0.045 ± 0.034	0.018	0.107
GT	0.020	0.005	0.016 ± 0.013	0.026 ± 0.023	0.010	0.073

Table I for the ideal A- and B-DNA sequences investigated here. For B-DNA, the T_{ij} value is much larger in poly(G) than in poly(A). Also, the electronic couplings for poly(GA) and poly(AT) are significantly larger compared with poly(A). In the case of ideal A-DNA, the relation is completely reversed which again confirms that T_{ij} is determined by DNA conformation.

Figure 2(a) shows the calculated transmission for various B-DNA sequences. The homogeneous sequences poly(A) and poly(G) show resonances at the eigenvalues of the corresponding Hamiltonian matrices. Due to the very small values of the electronic coupling parameters, these eigenvalues lie very close to the onsite energies of the respective base pairs (weak mixing). In heterogeneous sequences like poly(GA) and poly(GT) [We denote sequences where both A-T and G-C base pairs are present as heterogeneous; otherwise, if only one of the Watson-Crick pairs (WCPs) is present it will be denoted as homogeneous], the transmission is strongly reduced, which is due to the large energy gap between the AT and GC base pairs. The irregular Dickerson sequence also shows peaks at the energy levels of the AT and GC base pairs; however, the transmission is considerably reduced due to the large static disorder (different onsite energies along the chain).

The transmission functions $T(E)$ for different sequences follow roughly the absolute values of the electronic couplings for ideal B-DNA in Table I. Poly(G) shows clearly the largest transmission followed by poly(AT) and poly(GC). However, this is not true for heterogeneous sequences with a large static disorder, as is the case of poly(GT), for which the transmission is very different although the electronic couplings (see Table I) are rather similar to those of poly(A). We also calculated the corresponding *I-V* characteristics of various sequences, and these can be found in the supplementary material.[101]

2. Transport through fluctuating bridges: No solvent effects

The CT parameters are now evaluated along the MD trajectories as described above, omitting the QM/MM term (Q_A) in Eq. (7). In this case, the onsite energies ϵ_i fluctuate in the order of 0.15 eV,[42,43] driven by the skeletal modes of the DNA bases. The MD is performed for undecamers; however, to avoid end effects we analyze only seven sites from the core of the helix. Along these trajectories we calculate $\epsilon_i(t)$ and $T_{ij}(t)$ for the seven sites along the chain (in gas phase) and the transmission $T(E)$ for MD snapshots, which are saved every 1 ps. $T(E)$ is then averaged over these 30 000 events.

Table I shows the MD-averaged couplings in comparison to those of the ideal A- and B-DNA structures. In most cases, the MD averages $\langle T_{ij}\rangle$ deviate significantly from those of ideal sequences. Since the couplings depend sensitively on the DNA conformation, this suggests that the averaged MD structures are significantly different from the ideal ones, as discussed in detail before in Ref. 43. The role of fluctuations is further reflected in the variances σ, which are of the same order of magnitude as the averages themselves. These results are nearly independent of the interaction with solvent, indicating that the electronic coupling fluctuations are mainly dominated by the mutual orientation of the base pairs and are not sensitive to the electrostatic coupling to the environment.[43] Note, however, that the structure of DNA sensitively depends on salvation; therefore, the coupling parameters may be very different for simulations with varying solvation conditions.

Taking the value of $\langle T_{ij}\rangle$ as an indicator for a high or low transmission as a first approximation, we can sort the results in Table I for different sequences by $\langle T_{ij}\rangle$: poly(A) > poly(AT) > poly(GA) > poly(G) > poly(GT) > poly(GC). Therefore, the average transmission is dominated by the mean electronic coupling in these structures.

Figure 2(b) shows the transmission for various sequences. As a result of the broad distribution of the onsite energies, the transmission spectrum broadens. Further, the dynamical disorder of onsite energies increases the transmission of low-conducting (static) structures, while it decreases for "high-conducting" ones, as shown in Table II. This is a very interesting result and can be rationalized as follows: The fluctuations of onsite energies lead to conformations for "mixed" sequences such as poly(GA), poly(GT), and Dickerson, where the effective energy gaps become smaller than in the idealized static structures. Therefore, CT-active conformations arise due to the dynamics. On the contrary, the

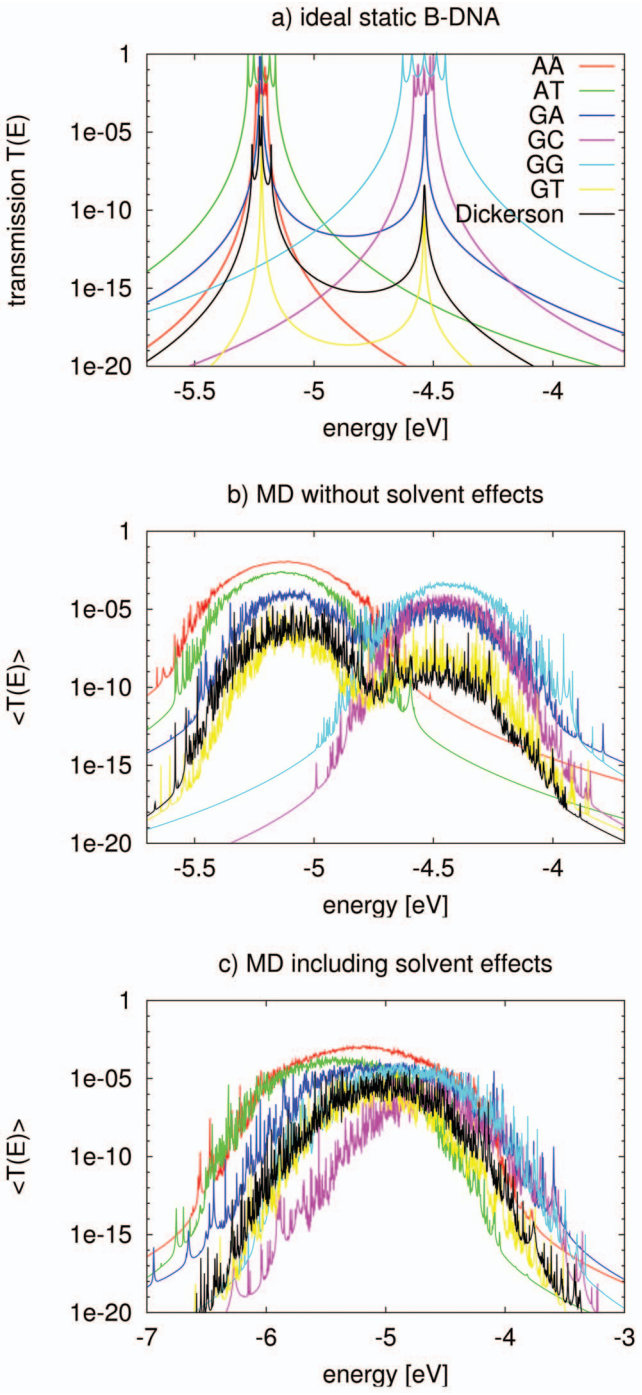

FIG. 2. (Color) (a) Transmission of the ideal chain including (b) dynamical effects and the (c) effect of environment for various DNA sequences. Note the broader energy range in (c).

homogeneous sequences become effectively disordered due to the dynamical fluctuations reducing the transmission. This point will be analyzed in more detail below.

3. Transport through fluctuating bridges: Influence of the DNA backbone, water, and counterions

To include the effect of DNA backbone, water, and counterions, the Hamiltonian in Eq. (7) is used to calculate the new electronic coupling and onsite energy parameters. The effect of environment on these parameters has been analyzed in detail in Ref. 43. The electric field induced by water molecules leads to large fluctuations of the onsite energies in the order of 0.4 eV compared to only 0.14 eV without the environment. Also the averages $\langle \epsilon_i \rangle$ are shifted by 0.2–0.3 eV to lower energies (see Table II in the supplementary material).[101] However, poly(A) seems to be the only exception with no significant energy shift. As already pointed out, the electronic couplings T_{ij} do not depend sensitively on the environment and are determined by the DNA conformation.

TABLE II. Maximum current values (at voltage $U=2$ V) for seven DNA heptamers sequences for static B-DNA structures for the average current $\langle I \rangle$ of the MD structures with and without QM/MM environment. All values are in nanoamperes.

Sequence	Static	Dyn. vacuo	Dyn. QM/MM
AA	202.0	215.7	47.75
AT	1019	39.06	6.404
GA	163.1	1.545	2.787
GC	299.2	0.647	0.086
GG	2511	6.502	1.644
GT	0.093	0.018	0.120
Dickerson[a]	0.023	0.043	0.251

[a]Eight base pairs instead of seven.

Figure 2(c) shows the transmission of the DNA species in the presence of electrostatic field induced by the environment. Since the environment does not affect the electronic coupling strongly, the main difference from Fig. 2(b) arises from the larger fluctuations of onsite energy values. As a result of the wider distribution of onsite energies as well as the environment-induced energy shifts, the transmission spectra become considerably broader and the clear separation into two transmission subsets found in Fig. 2(b) is now blurred out. In principle, the transport properties of various sequences seem to become more similar to each other than it was the case for the static B-DNA, suggesting that the sequence dependence becomes less important. The current values in Table II also show that the differences in charge transport between various sequences decrease when including the dynamical and environmental effects. For static B-DNA structures, there is a difference of 4–5 orders of magnitude in the current between the poly(G) and Dickerson sequence. However, this sequence dependence decreases dramatically in the full dynamics (dyn. QM/MM), where the current values lie in a range of 1–2 orders of magnitude. This effect may be related to the experimental results obtained in the studies[44] and in Ref. 29. As described in Sec. I, very similar currents were obtained in both experiments despite the completely different sequences.

Interestingly, poly(A) shows the largest transmission in contrast to the static case where poly(G) is better conducting. This can be related to the changes in molecular conformation, which make the average coupling increase. Indeed, there is a strong relationship between the average electronic couplings $\langle T_{ij} \rangle$ in Table I and the average transmission $\langle T(E) \rangle$ in Fig. 2(c). The order of the $\langle T(E) \rangle$ maxima or, more quantitatively, the $I(U)$ values in Table II for the studied sequences is poly(A) $\gg$ poly(AT) $>$ poly(GA) $>$ poly(G) $\gg$ Dickerson $>$ poly(GT) $>$ poly(GC) and is therefore in good agreement with the order of the corresponding average elec-

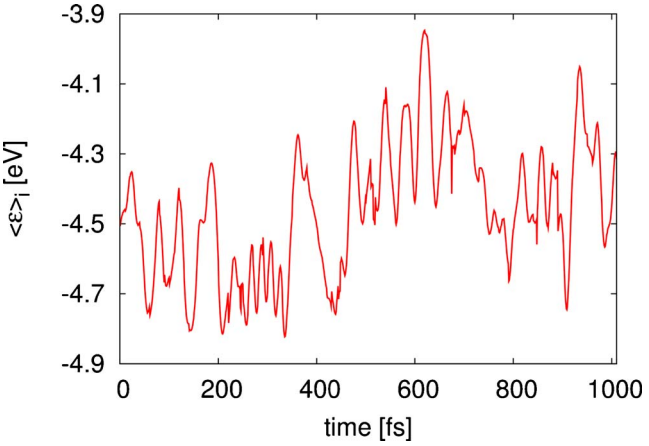

FIG. 3. (Color online) Time-dependent average over onsite energies $\langle \epsilon(t) \rangle = (1/N)\Sigma_j \epsilon_j(t)$ obtained from a 100 ps MD simulation of a poly(G) heptamer ($N=7$). Snapshots were recorded every femtosecond.

tronic couplings. This shows that $\langle T_{ij} \rangle$ is a good indicator for transport properties of DNA species, characterizing the entire ensemble of molecular structures with their very different individual T_{ij} values.

Particularly interesting is the transmission of the heterogeneous species such as poly(GA), poly(GT), and the Dickerson structure, which contain both types of Watson–Crick pairs A-T and G-C. Here, the transmission increases substantially compared to the idealized static case, indicating that the fluctuations of onsite energies may lead to conformations with smaller effective onsite disorder. The increased conductance of the heterogeneous sequences can also be seen in Table II. For all three of them, even for poly(GA), the average current $\langle I \rangle$ becomes larger if the electrostatic environment of DNA is considered. This confirms the previous statement, and moreover, it suggests that besides the average electronic couplings also the strong fluctuations of onsite energies seem to play a very important role for charge transport in DNA.

The width of $\langle T(E) \rangle$ in Fig. 2(c) shows that the energy range for transmissive conformations becomes much larger than it was the case in Fig. 2(b) and even more so in Fig. 2(a). For instance, the energy range for poly(A) where $\langle T(E) \rangle$ is larger than 10^{-5} is 1.7 eV compared to 0.7 eV without environment and only 0.05 eV in the static case [Although one should notice that the maxima in the transmission decrease from Fig. 2(a) to Fig. 2(b) and also from Fig. 2(b) to Fig. 2(c) at least for most of the studied sequences]. However, this indicates that the onsite energy fluctuations are not always completely disordered and therefore destructive, i.e., sometimes they can lead to transmissive conformations for very different energies. The effect can also be followed by computing the average onsite energy $\langle \epsilon(t) \rangle = (1/N)\Sigma_j \epsilon_j(t)$ along the poly(G) heptamer ($N=7$) for every snapshot along the MD simulation, as shown in Fig. 3. The onsite energies seem to undergo collective fluctuations in the range of 1 eV, which again explains the large broadening of the transmission function, i.e., conducting conformations at various energies are explored during the time evolution of the system. These calculations demonstrate that it is not meaningful to consider averages for onsite energies (ionization potentials). Therefore, the charge transport properties of a DNA species cannot be traced back to the averaged onsite energies in any way.

To analyze the effect of disorder for both ϵ_i and T_{ij} in more detail, we have performed additional sets of calculations. We calculated $\langle T(E) \rangle$ for all nine possible combinations, where ϵ_i or T_{ij} were (i) fixed at their idealized B-DNA values, (ii) fixed at their MD averages, or (iii) free to fluctuate. The calculations suggest that the time averages of T_{ij} determine the average transmission but the fluctuations of electronic couplings have only a small impact. On the other hand, taking the averages of onsite energies does not seem to be appropriate for such kind of transport calculations. Instead, our results indicate that the fluctuations of ϵ_i have a large impact on the average transmission. They can either hinder or facilitate the transport, which depends on the "initial" static onsite disorder. The complete results of this analysis can be found in the supplementary material.[101] We may thus conclude that the real values of T_{ij} may be substituted by the respective mean values in the calculation of transmission. Of course, the transmission at each time step depends sensitively on the corresponding electronic coupling, but the average transmission is dominated by the mean electronic coupling. In contrast, the fluctuations of onsite energies cannot be replaced by the average onsite energies because the transmission is dominated by a few configurations with CT-favorable onsite energies. This will be analyzed in more detail below.

4. Length dependence

Here, we investigate how the transport properties of DNA are influenced by the length, i.e., the number of sites. For this purpose we carried out 30 ns MD simulations of poly(G) and poly(A) DNA with up to 31 base pairs. In Fig. 4 we show the average transmission values for various DNA length at two constant arbitrary energies which are (i) the average onsite energies $\langle \epsilon \rangle$ and (ii) separated by a gap of 1.5 eV from $\langle \epsilon \rangle$ for poly(A) and poly(G), respectively. We clearly see that there is an exponential decay of transmission with increasing number of sites. This is what we would expect since more sites lead to larger dynamical disorder in the electronic parameters. Because of that, the probability of conformations with sufficiently large T_{ij} and also similar ϵ_i along the chain becomes smaller with increasing number of sites. The exponential decay of transmission has the form $T(E=\text{const}) = Ae^{-\beta L}$ where β describes the intensity of decay and the distance $L=Nd$ (N is the number of base pairs and d is the stacking distance of ~3.4 Å).

However, the exponential decay of transmission is considerably stronger for energies which are separated from $\langle \epsilon \rangle$ by a large gap. From Fig. 4, we can extract decay parameters β for the latter case ($\langle \epsilon \rangle + 1.5$ eV), which are 0.77 Å^{-1} for poly(A) and 0.98 Å^{-1} for poly(G), respectively. On the other hand, we get substantial smaller β-values for the former case ($\langle \epsilon \rangle$). Here, β takes the values of 0.22 Å^{-1} for poly(A) and 0.36 Å^{-1} for poly(G), indicating some kind of lower limit for the decay of transmission. Recently, Berlin *et al.*[102] re-

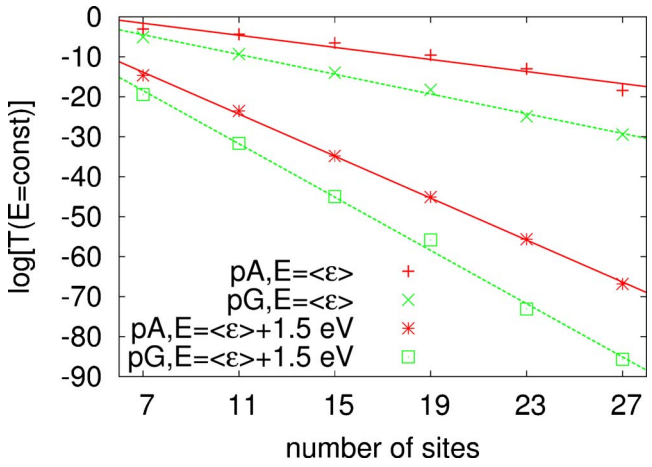

FIG. 4. (Color online) Length dependence of $\langle T(E)\rangle$ for poly(G) and poly(A). Shown are logarithmic transmission values for various DNA length, i.e., number of sites N at two constant arbitrary energies which are the average onsite energies $\langle\epsilon\rangle$ and $\langle\epsilon\rangle+1.5$ eV for poly(A) and poly(G), respectively. The data points were fitted by functions of the form $T(E=\text{const})=Ae^{-\beta L}$ where $L=Nd$ (d is the stacking distance of ~3.4 Å) and β describes the decay rate of transmission. For poly(G) β is 0.36 Å^{-1} and for poly(A) 0.22 Å^{-1} at $E=\langle\epsilon\rangle$. However, if an energy gap of 1.5 eV to $\langle\epsilon\rangle$ is present both β-values increase to 0.77 and 0.98 Å^{-1} for poly(A) and poly(G), respectively. In both cases the exponential decay of transmission in poly(G) is stronger than in poly(A). The complete $\langle T(E)\rangle$ curves for the different lengths can also be found in the supplementary material (Ref. 101).

ported that there is a minimum value of the decay parameter β in the tunneling regime which is 0.2–0.3 Å^{-1}.

Irrespective of the given energy, the length dependence of transmission is significantly stronger in poly(G) than in poly(A). This may be due to different average electronic couplings, which are 0.03 eV for poly(G) and nearly 0.06 eV for poly(A) (see Table I). No significant changes in the electronic parameters ϵ_i and T_{ij} with increasing DNA length were found (see also supplementary material).[101]

B. The role of DNA dynamics and coherent motion on charge transfer efficiency

Many theoretical studies of DNA conduction have approximated the dynamical and solvent effects using statistical models.[45,46,57,103,104] Here, we compare the results from the MD simulations of a poly(A) heptamer with those obtained by two statistical models. As has been shown before,[43] the fluctuations of onsite energies exhibit strong correlations between the sites, which may have an impact on conduction. These correlations may be induced by the motion of solvent water molecules, which have been shown to introduce fluctuations of the onsite energies with a period of 40 fs. The water modes introduce a periodically fluctuating potential at the DNA base sites, which lead to the fluctuation of onsite energies. A possible explanation for this correlation effect is that neighboring sites see similar electrostatic potentials. As mentioned above, the distributions of ϵ_i and T_{ij} resulting from classical MD simulations are normal. To discard the correlations of adjacent sites along the DNA chain, we define a statistical model which is called "PDF (probability distribution function)." In this model, the onsite energies are taken randomly from normal distributions $P(\epsilon_i)$ for each site i of the chain. These distributions are obtained directly from the

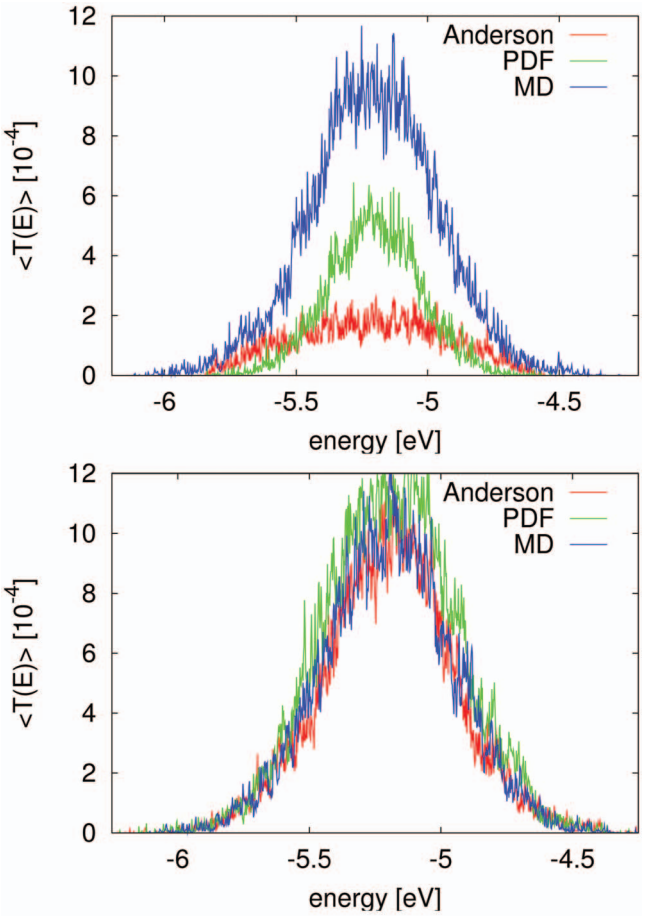

FIG. 5. (Color) Comparison of $\langle T(E)\rangle$ for the MD simulation of a poly(A) heptamer with two statistical models. Top panel: The electronic couplings for the three models are set to 0.05 eV. The average transmission function is calculated for onsite energies from the MD simulation time series (blue); for onsite energies drawn from the respective probability distribution functions on each site (green); and the Anderson model (red) where all onsite energies are randomly drawn from a square-box distribution. Bottom panel: Now the original MD time series of onsite energies is used, the same for the three models, while $\langle T(E)\rangle$ is calculated for electronic couplings T_{ij} from the original MD time series (blue); for T_{ij} drawn from their respective probability distribution functions (green) and the Anderson model (red), respectively. The used probability distribution functions for ϵ_i and T_{ij} are shown in the supplementary material (Ref. 101).

corresponding MD simulation of the respective DNA species. This ensures that a realistic onsite energy distribution for each site is used while time correlations between the sites are not present. The third model is based on the Anderson[105] model of disorder, where the onsite energies are randomly drawn from a square-box distribution of width w with uniform probability $P(\epsilon)=1/2w$. The box width is $w=\sqrt{3}\sigma$, where $\sigma(\epsilon)$ is the standard deviation of onsite energies resulting from MD simulations ($\sigma\sim0.4$ eV).

To make the results comparable, the electronic couplings are taken at constant $T_{ij}=0.05$ eV, since as shown above, the fluctuations of T_{ij} have only a minor influence on the conduction. The average transmission of poly(A) heptamer for the two models and the full MD simulation is shown in the top panel of Fig. 5. The three spectra have the same position of maxima, since the transmission functions originate from the distributions of onsite energies, which are all symmetric with the same mean value. Clearly, the Anderson model

largely underestimates the transmission, showing the importance of proper MD sampling of the right distribution of charge transfer parameters. However, also the PDF model based on MD trajectories but neglecting nonlocal correlations reproduces only half of the transmission as found for the full MD simulation. As has been discussed in detail previously,[43] the fluctuations of onsite energies of neighboring sites are highly correlated with a correlation coefficient of about 0.7. Even second neighbors exhibit a significant correlation. Therefore, due to this correlated motion of the onsite energies a picture emerges, where the onsite energies in a region of 3–5 bases undergo concerted motion, which is not taken into account in the PDF and Anderson models. This correlated dynamics leads to a distribution of onsite energies, which has less disorder on average.

As shown in the bottom panel of Fig. 5, the choice of T_{ij} has only a minor effect on the transmission, which means there is no correlation between the couplings which is important for transport. The comparison of both plots shows that the choice of T_{ij} at a reasonable constant value [here 0.05 eV, roughly the MD average of poly(A)] gives nearly the same average transmission as taking the real time series from MD. Therefore, we conclude that the charge transport efficiency depends strongly on onsite energies, which are determined by the environment. Furthermore, our results indicate that DNA charge transport models, in which energetics is based on statistical distributions, do not include nonlocal correlation between adjacent sites, and therefore they miss an important contribution to the charge transport. The corresponding *I-V* characteristics can be found in the supplementary material.[101]

C. Conformational analysis

Is this section, we analyze the effect of disorder on transmission for both electronic parameters ϵ_i and T_{ij} along the DNA chain in more detail. One of the goals is to estimate the amount of conformations which are active for charge transport. The so-called coherence parameter has been analyzed recently in the context of electron transfer in proteins in aqueous solution in order to understand the effect of fluctuations on charge transfer in more detail.[106] We used the notion of coherence parameter and applied it to the transmission function and the collective couplings along the DNA chain. The results can be summarized as follows: (i) The coherence parameter for the transmission function is much smaller than 1, which indicates that fluctuations dominate the transport, i.e., strong dynamical disorder; (ii) the coherence parameter for the transmission is larger in poly(A) than in poly(G) which may be the source of better conductance in poly(A); (iii) most of the dynamical disorder is due to the onsite energies; and (iv) coherence parameter for collective electronic couplings along the DNA chain is much closer to 1, indicating once again that the averages of T_{ij} still affect the charge transport in contrast to ϵ_i. The full data for this analysis are presented in the supplementary material.[101]

For a further analysis of the role played by conformational dynamical disorder, we propose two simple measures for the onsite and hopping disorder along the DNA chain, respectively

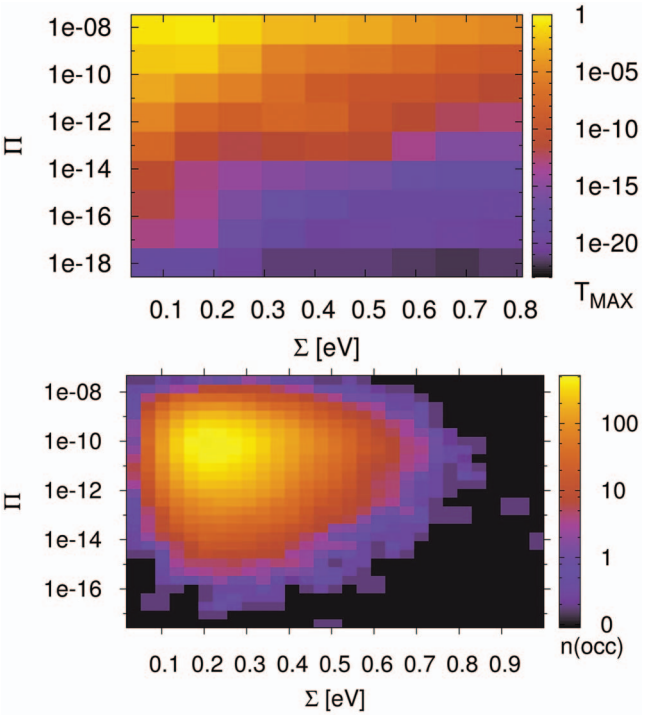

FIG. 6. (Color) Statistical analysis of $T_{\max}$ in a poly(G) heptamer for the 30 ns data with electronic parameters for every picosecond (30 000 DNA conformations). $T_{\max}$ depending on Σ and Π (top); number of conformations found in a given interval of Σ and Π (bottom).

$$\Sigma = \sqrt{\frac{1}{N}\sum_{i=1}^{N}(\epsilon_i - \langle\epsilon\rangle_N)^2} = \sqrt{\langle\epsilon^2\rangle_N - \langle\epsilon\rangle_N^2}, \tag{13}$$

$$\Pi = \prod_{i=1}^{N-1} T_{i,i+1}. \tag{14}$$

The standard deviation Σ is calculated for the ϵ_i along the chain and has an evident meaning. Large values of Σ indicate large differences of neighboring site energies. Note that the index N in $\langle\epsilon\rangle_N$ and $\langle\epsilon^2\rangle_N$ means that averaging is performed for the N sites along the chain. The other parameter Π is motivated by the form of Green's function matrix element $G_{1N}(E)$ required to calculate the transmission function, which scales approximately as the product of electronic couplings. Thus, this quantity determines the transmission efficiency of the system; small values of Π account for conformations with small couplings along the DNA chain. In order to reduce the complexity of further analysis we additionally define the value $T_{\max}$ as simply the maximum of a given transmission function $T(E)$. Note that the value $T_{\max}$ can be located anywhere within the respective energy range. All three parameters Σ, Π, and $T_{\max}$ are now calculated for 30 000 snapshots along the 30 ns MD trajectory of a poly(G) heptamer.

The results are shown in Fig. 6 (top panel). We see that none of the measures Σ and Π alone is able to describe the conformations of high conduction, but both seem to contrib-

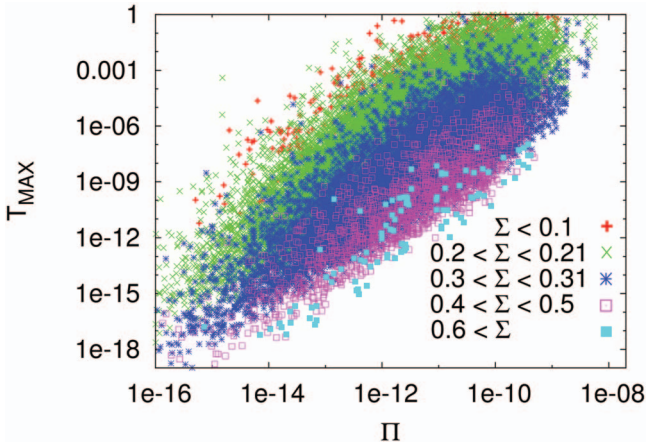

FIG. 7. (Color) Plot of T_{max} depending on Π for fixed values of Σ based on the same data as used in Fig. 6.

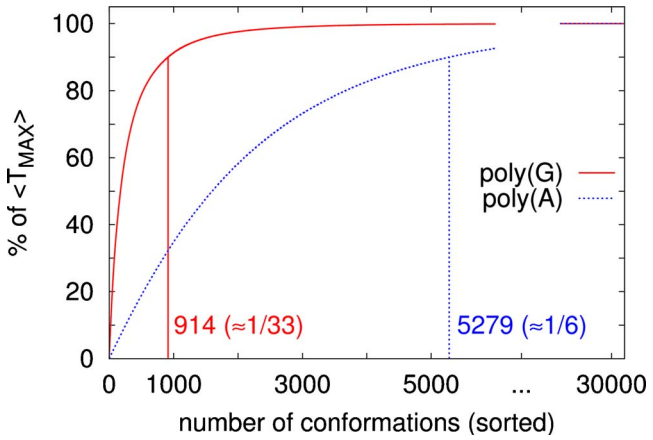

FIG. 8. (Color online) Conformational analysis: The amount of conformations that make up 90% of $\langle T_{max}\rangle$; calculation of electronic parameters with QM/MM-environment for every picosecond snapshot along the 30 ns MD simulation; comparison between poly(G) and poly(A) heptamers; the T_{max} values are sorted beginning with the largest.

ute nearly linearly to the transmission (note the logarithmic scales for Π and T_{max}). However, for the transport active conformations, small Σ and large Π values are required.

Figure 6 (top panel) also shows that T_{max} depends more strongly on Π than on Σ. For instance, if Π is kept fixed at 10^{-8}, then the maximum transmission T_{max} is still at least 10^{-7} for all values of Σ. On the other hand, keeping the parameter Σ fixed makes T_{max} decrease to almost 10^{-17} even for the smallest value of Σ. Figure 6(bottom panel) shows the corresponding occupation plot. Here, we quantify how many conformations exhibit a certain combination of Σ and Π parameters. It seems that the number of transport active conformations with appropriate electronic couplings and onsite energies is very small. The most conformations have Π values of about 10^{-10} and Σ values of about 0.25 eV and are therefore "CT-silent."

To study the effects of both parameters Σ and Π in detail, we plot T_{max} against Π for fixed values of Σ. Figure 7 again indicates that there is a linear relation between log(Π) and log(T_{max}), although the data points are largely spread. For various Σ, the data sets are nearly parallel to each other, merely shifted along the *y*-axis due to different Σ values. A small Σ means less dynamical onsite disorder and leads to larger T_{max} values. As can be seen from the values in Table III, the correlation coefficient between log(Π) and log(T_{max}) for full MD takes quite a large value of 0.76. The correlation even increases to 0.84 when Σ is fixed. Keeping Π fixed leads to a marked anticorrelation of −0.68.

This clearly demonstrates that if we deal with instantaneous transport for a single DNA conformation, then the charge transport is indeed affected very strongly by the actual electronic parameters, especially the electronic couplings. At this point, it is important to stress that these results are by no means in contradiction to those obtained in Sec. I: We showed that the transport on average depends only on the average electronic couplings.

TABLE III. Correlation coefficient $\rho(X,Y)$ of log(T_{max}) with log(Π) and Σ.

X	*Y*	QM/MM	Vacuo	Fixed Σ	Fixed Π
log(Π)	log(T_{max})	0.76	0.79	0.84	⋯
Σ	log(T_{max})	−0.47	−0.33	⋯	−0.68

As already shown in Fig. 6 (bottom panel) there are a very few charge transport active conformations. To put this in a more quantitative way, we proceed as follows: (i) Sort the 30 000 T_{max} values for the whole MD trajectory beginning with the largest; (ii) calculate the total average transmission maximum $\langle T_{max}\rangle$; and (iii) determine how many of the best-transmissive conformations are necessary to obtain 90% of $\langle T_{max}\rangle$. Figure 8 shows the conformational analysis for the poly(A) and poly(G) heptamers. In the latter case, only 914 of 30 000 conformations are active for charge transport, i.e., on average only every 33rd conformation. In poly(A), the number of significantly contributing structures increases dramatically to 5279 (on average every sixth). Thus, the difference in conductance between poly(A) and poly(G) can be related to these results, which are in good agreement with the calculations of respective coherence parameter. The average transport in both sequences is dominated by the dynamical disorder, i.e., only a few conformations contribute to transport. However, the dynamical disorder in poly(G) is considerably larger than in poly(A). For the charge transport active conformations, the mean values of Σ and Π are 0.20 eV and 1.34×10^{-7} for poly(A) and 0.19 eV and 3.23×10^{-9} for poly(G), respectively.

Interestingly, dynamical fluctuations can hinder or support charge migration. The latter case occurs in cases where the transmission is small in the static structure; structural fluctuations bring on transmission-active conformations with small Σ values. For instance, the Dickerson sequence, where the average T_{ij} are not small (see Table I), profits very much from the fluctuations. As shown in Fig. 9, the interaction with the environment suppresses the CT-active conformations and thereby the transmission in poly(G). On the other hand, the number of CT-active conformations in the Dickerson sequence is increased. This can be seen in the Σ-value, which is 0.35 eV for the static structure and decreases to 0.25 eV as an average of the CT-active conformations in the

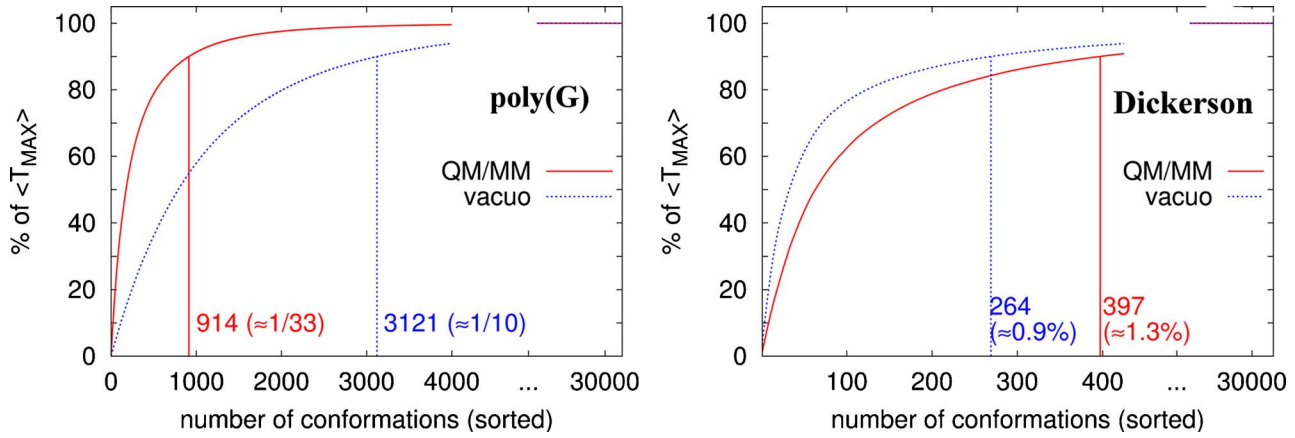

FIG. 9. (Color online) Conformational analysis: The amount of conformations that make up 90% of $\langle T_{max} \rangle$ based on the calculation of electronic parameters with QM/MM environment and *in vacuo*. Comparison between the homogenous poly(G) heptamer (left) and the central heptamer of the heterogeneous Dickerson sequence (right). The T_{max} values are sorted beginning with the largest.

QM/MM dynamics. Note that due to initial differences in the static disorder (different onsite energies along the chain) the number of transport active conformations in poly(G) is generally larger than in the heterogeneous Dickerson sequence.

D. Time scales and averaging for CT in DNA

Up to now, we have primarily focused on a statistical analysis of the transmission function averaged over snapshots from 30 ns MD simulations. The analysis clearly showed the existence of charge transport active conformations; however, nothing has been said about time scales of ionic and electronic motion relevant for the transport, i.e., the question about averaging arises.

Büttiker and Landauer[107] analyzed a fluctuating model potential in order to determine tunneling traversal times, i.e., the time a particle spends in passing a barrier with height V_0 and fluctuation with $V_1 \cos(\omega t)$. For low frequencies ω, the particle experiences a static barrier, while high frequencies (compared to the tunneling time) lead to a time averaging of the potential, i.e., the particle effectively sees the mean potential $V_0 + \langle V_1 \rangle$. Recently, a detailed analysis of ionic (τ_1) and electronic (τ_2) time scales on the charge transfer in donor-bridge-acceptor systems has been performed.[102] For slow dynamic fluctuations (structural fluctuations with characteristic time τ_1), a nonexponential time evolution of the CT process has been reported caused by the configurational averaging of the electronic parameters. The averaging performed above would address this situation. However, a few CT-active conformations would enhance/dominate the whole charge transfer. A similar picture emerged, e.g., from the analysis of electron tunneling through water.[108] For fast dynamic fluctuations, $\tau_1 \ll \tau_2$, on the other hand, the self-averaging of the electronic parameters as in Ref. 107 leads to a static correction to the time independent rate constant.[102]

Therefore, the question arises how to average the transmission in the case of DNA where fluctuations are large and perturbation theory may not be applicable. Consider, e.g., the case of poly(A): Here, in the idealized B-DNA conformation no barrier exists, i.e., there is no V_0 as in the model of Büttiker and Landauer.[107] Averaging increases the transmission continuously with the applied averaging time, as shown in Fig. 10. For long averages, the transmission of the ideal structure is retained. This could be expected since the time average of the onsite energies is nearly equal to those of the ideal structure, i.e., long time averages lead to a barrier-free situation.

For poly(GT), in contrast, averaging decreases the transmission continuously, as shown in Fig. 10. Again, the aver-

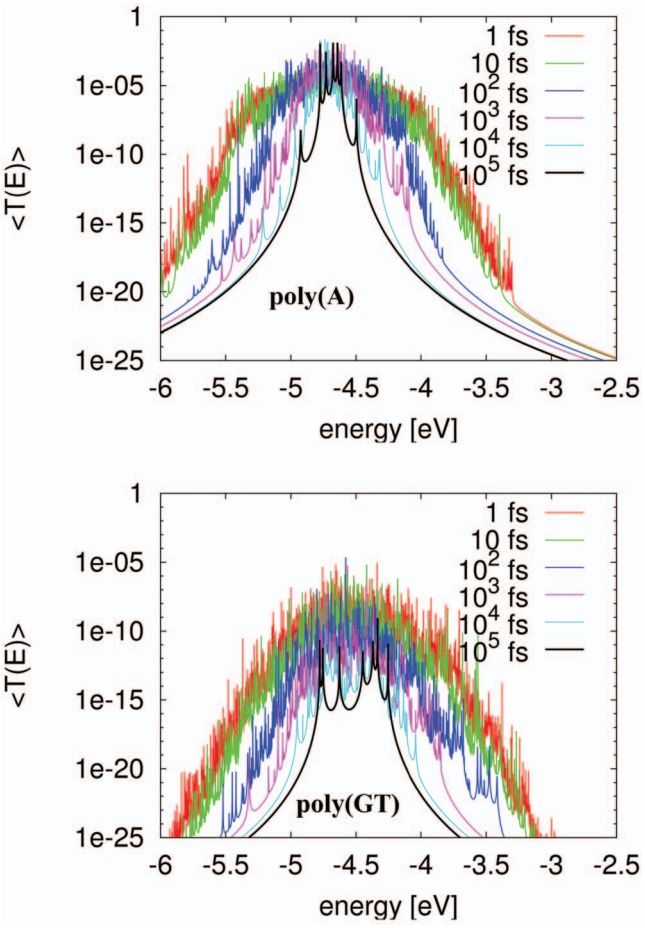

FIG. 10. (Color) Average transmission for various sets of averaged electronic parameters for poly(A) (top) and poly(GT) (bottom). Both of them obtained from 100 ps MD data with a time step of 1 fs.

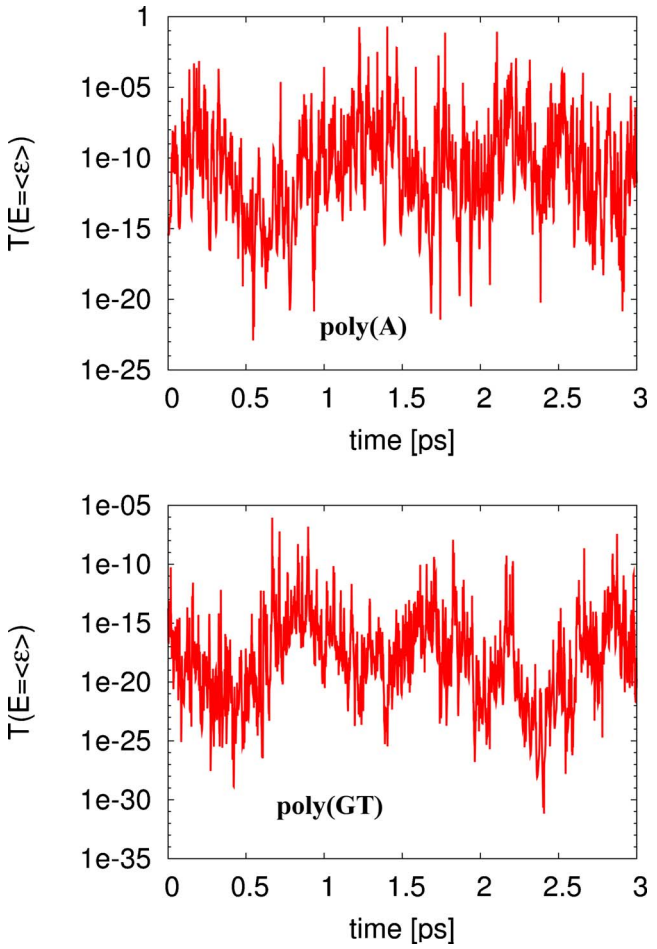

FIG. 11. (Color online) Snapshot of a 3 ps time series for the transmission at $E=\langle\epsilon\rangle$ for poly(A) (top) and poly(GT) (bottom), respectively, based on the simulation data as used in Fig. 10.

ages resemble the situation of the ideal structure, thereby deleting the CT-active conformations. These two examples show that fluctuations can act in different directions, increasing or decreasing the transmission or CT rate. Troisi *et al.*[109] derived an expression for the rate constant for CT through fluctuating bridges. The correction to the static limit takes into account the coherence parameter in a unique way. This, however, may not be applicable for DNA, since here the effect of fluctuations does not affect the CT in the same way.

The averaging problem shows that time scales should be carefully discussed in the context of DNA. The time scales for ionic motion, which are important for CT, are not easy to determine. The Fourier transform of the autocorrelation function of time series of CT parameters showed a multitude of modes:[43] The DNA-base skeletal motion with a period of 20 fs, the "water" mode with a period of 40 fs, and the motion of counterions and the DNA backbone, which are 1 ps and longer. It is difficult, however, to asses their relative importance on the transmission. Figure 11 shows a time series of the transmission for poly(A) and poly(GT). Larger fluctuations in the picosecond regime are modulated by much smaller fluctuations in the femtosecond regime. The fast fluctuations span quite a large range of transmission; however, it seems that the maxima of the picosecond time fluctuations indicate the existence of charge transfer active conformations, which are persistent for a short time. In this time, an averaged potential may be assumed as in the analysis of Büttiker and Landauer, which may allow to compute the amount of charge transferred during the CT-active conformation. Additional analyses showing the relation between time domains of large transmission and the transferred charge in time can be found in the supplementary material[101] (Fig. 11). The analysis of a window of 100 ps shows the appearance of CT-active conformations on even longer time scales, i.e., the picosecond oscillations, as shown in Fig. 11, are only a modulation on structural modifications on a longer time scale. For poly(A), e.g., during a period of 60 ps, three distinct regions appear with high transmission, which leads to an increased charge transfer as competed as the integrated current. A very similar picture arises for poly(GT). According to this analysis, a considerable fraction of charge is transported on a picosecond time scale. However, it is not clear how to separate the time scales τ_1 and τ_2 in the case of DNA. From the analysis above it looks like as if the conformations determine the CT, i.e., there is a conformational gating situation in that the ionic conformation allows or blocks the CT. The CT "open" conformations are then further modulated by fast fluctuations in the femtosecond regime, in particular, the water modes, which are important to understand the transmission quantitatively, as analyzed in Secs. III A–III C.

IV. DISCUSSION AND CONCLUSIONS

The SCC-DFTB-FO approach[42] allows to calculate the conduction properties of DNA using a realistic representation of dynamical and environmental effects. Our simulations highlight several aspects crucial to understand the transport properties of DNA oligomers, which are not easy to capture with simple model Hamiltonians.

First of all, the DNA conformation is critically determined by the presence of solvent, i.e., it can deviate significantly from the static A- or B-DNA structure. This has a large impact on the off-diagonal charge transfer parameters T_{ij}, making their average values deviate significantly from those of the static DNA forms. Therefore, any study of DNA conduction should be based on structures generated from all-atom MD simulations rather than idealized structures. The fluctuations of T_{ij} are determined by the conformation of the DNA, whereas the solvent has a negligible influence.[43] Our analysis shows that the charge transport under given conditions depends sensitively on the average values of electronic coupling parameters only. In our view, there is no need to assume any coherent motion of DNA, which would enhance charge transfer, as proposed recently by Reha *et al.*[110] Nevertheless, the T_{ij} critically determine the transmission.

On the other hand, of crucial importance are the fluctuations of onsite energies. Those are in the order of 0.4 eV and can thereby introduce large barriers for tunneling along the DNA. Interestingly, the effect of fluctuations is opposite for sequences with low and high static disorders. For instance, in poly(G), the onsite dynamical disorder reduces the number of CT-active conformations dramatically. In contrast, in structures with high static disorder (Dickerson DNA), high transmission structures are introduced, which increase the

average transmission significantly. In general, we see that the sequence dependence becomes less important than in the static structures, which is in agreement with experimental observations of similar currents obtained for completely different DNA sequences.[29,44] In the light of our results, the charge transport based on Landauer theory is a highly nonequilibrium process, i.e., only few conformations contribute to transmission. These conformations are characterized by a small Σ-value, i.e., all onsite energies are nearly equal. Clearly, this situation cannot be described by the mean values of onsite energies because there is no direct link between the averages of onsite energies and the charge transport properties in contrast to the averages of electronic couplings.

As we have shown before, the fluctuations of onsite energies are determined by the modes of solvent water.[43] These water modes are also responsible for the correlated motion of onsite energies, which we have shown to be important for transport as well. The correlation increases the maximal transmission and the current by a factor of 2 and 3 and 4, respectively.

Several mechanisms of charge transfer in DNA concerned with dynamical effects have been proposed over the years. One of them is the counterion-gating model[111] which suggests that the motion of counterions triggers the charge transfer. We have shown that the effect of counterions cannot be separated from the motion of water and DNA. Since water motion counteracts the ion motion, the transport cannot be traced back to the dynamics of single ions.[43] Nevertheless, the time series of the transmission shows significant fluctuations in the picosecond regime. Therefore, the correlated motion of ions and water may introduce CT-active conformations, which are important to understand CT in DNA. O'Neil and Barton[6] suggested a model where the CT-active DNA conformations are determined by large values of Π. Our analysis confirms the basic intuition of CT-active conformations. However, rather than the DNA conformation with good stacking contacts leading to large Π values, conformations with small Σ may be more important. The reason is that average conformations lead to average Π values, which are large enough for sufficient transmission. The alignment of onsite energies, on the other hand, is the critical condition which "gates" the charge transport. Further, the dynamics of onsite energies is determined by the solvent as the large change in the transmission due to the inclusion of solvent and ions indicates. The concerted motion of DNA, water, and ions brings on CT-active situations. However, it is quite difficult to separate the impact of each factor. The importance of the solvent suggests that it is rather "water gating" than conformational gating[6] which drives the charge transport in DNA.

ACKNOWLEDGMENTS

This work was supported by the Deutsche Forschungsgemeinschaft (Project No. DFG-EL 206/5-1), the Deutsche Forschungsgemeinschaft under Contract Nos. CU 44/5-2 and CU 44/3-2, and by the South Korea Ministry of Education, Science and Technology Program "World Class University" under Contract No. R31-2008-000-10100-0.

[1] *Introducing Molecular Electronics*, Lecture Notes in Physics Vol. 680, edited by G. Cuniberti, G. Fagas, and K. Richter (Springer, New York, 2005).
[2] K. Keren, R. S. Berman, E. Buchstab, U. Sivan, and E. Braun, Science **302**, 1380 (2003).
[3] E. Braun, Y. Eichen, U. Sivan, and G. Ben-Yoseph, Nature (London) **391**, 775 (1998).
[4] M. Mertig, R. Kirsch, W. Pompe, and H. Engelhardt, Eur. Phys. J. D **9**, 45 (1999).
[5] S. O. Kelley and J. K. Barton, Science **283**, 375 (1999).
[6] M. A. O'Neil and J. K. Barton, J. Am. Chem. Soc. **126**, 11471 (2004).
[7] C. R. Treadway, M. G. Hill, and J. K. Barton, Chem. Phys. **281**, 409 (2002).
[8] C. J. Murphy, M. R. Arkin, Y. Jenkins, N. D. Ghatlia, S. H. Bossmann, N. J. Turro, and J. K. Barton, Science **262**, 1025 (1993).
[9] N. J. Turro and J. K. Barton, JBIC, J. Biol. Inorg. Chem. **3**, 201 (1998).
[10] E. M. Boon and J. K. Barton, Curr. Opin. Struct. Biol. **12**, 320 (2002).
[11] C. Wan, T. Fiebig, S. O. Kelley, C. R. Treadway, and J. K. Barton, Proc. Natl. Acad. Sci. U.S.A. **96**, 6014 (1999).
[12] S. O. Kelley, N. M. Jackson, M. G. Hill, and J. K. Barton, Angew. Chem., Int. Ed. **38**, 941 (1999).
[13] B. Giese, Annu. Rev. Biochem. **71**, 51 (2002).
[14] E. Meggers, M. Michel-Beyerle, and B. Giese, J. Am. Chem. Soc. **120**, 12950 (1998).
[15] F. D. Lewis, T. Wu, Y. Zhang, R. L. Letsinger, S. R. Greenfield, and M. R. Wasielewski, Science **277**, 673 (1997).
[16] F. D. Lewis, R. L. Letsinger, and M. R. Wasielewski, Acc. Chem. Res. **34**, 159 (2001).
[17] D. Ly, L. Sanii, and G. B. Schuster, J. Am. Chem. Soc. **121**, 9400 (1999).
[18] P. T. Henderson, G. Hampikian, D. Jones, Y. Kan, and G. B. Schuster, Proc. Natl. Acad. Sci. U.S.A. **96**, 8353 (1999).
[19] *Long-Range Charge Transfer in DNA I and II*, Topics in Current Chemistry Vol. 237, edited by G. B. Schuster (Springer, New York, 2004.
[20] B. Giese, S. Wessely, M. Spormann, U. Lindemann, E. Meggers, and M. E. Michel-Beyerle, Angew. Chem., Int. Ed. **38**, 996 (1999).
[21] J. Jortner, M. Bixon, T. Langenbacher, and M. E. Michel-Beyerle, Proc. Natl. Acad. Sci. U.S.A. **95**, 12759 (1998).
[22] M. Bixon, B. Giese, S. Wessely, T. Langenbacher, M. E. Michel-Beyerle, and J. Jortner, Proc. Natl. Acad. Sci. U.S.A. **96**, 11713 (1999).
[23] D. Porath, G. Cuniberti, and R. D. Felice, *Charge Transport in DNA-based Devices*, edited by G. Schuster (Springer, Berlin/Heidelberg, 2004), Vol. 237, p. 183.
[24] R. G. Endres, D. L. Cox, and R. R. P. Singh, Rev. Mod. Phys. **76**, 195 (2004).
[25] A. J. Storm, J. V. Noort, S. D. Vries, and C. Dekker, Appl. Phys. Lett. **79**, 3881 (2001).
[26] D. Porath, A. Bezryadin, S. D. Vries, and C. Dekker, Nature (London) **403**, 635 (2000).
[27] K.-H. Yoo, D. H. Ha, J.-O. Lee, J. W. Park, J. Kim, J. J. Kim, H.-Y. Lee, T. Kawai, and H. Y. Choi, Phys. Rev. Lett. **87**, 198102 (2001).
[28] B. Xu, P. Zhang, X. Li, and N. Tao, Nano Lett. **4**, 1105 (2004).
[29] H. Cohen, C. Nogues, R. Naaman, and D. Porath, Proc. Natl. Acad. Sci. U.S.A. **102**, 11589 (2005).
[30] J. Jortner, M. Bixon, T. Langenbacher, and M. Michel-Beyerle, Proc. Natl. Acad. Sci. U.S.A. **95**, 12759 (1998).
[31] J. Jortner, M. Bixon, A. A. Voityuk, and N. Rösch, J. Phys. Chem. A **106**, 7599 (2002).
[32] L. Blancafort and A. A. Voityuk, J. Phys. Chem. A **110**, 6426 (2006).
[33] A. Voityuk, N. Rösch, M. Bixon, and J. Jortner, J. Phys. Chem. B **104**, 9740 (2000).
[34] A. A. Voityuk, J. Chem. Phys. **128**, 115101 (2008).
[35] T. Cramer, S. Krapf, and T. Koslowski, J. Phys. Chem. C **111**, 8105 (2007).
[36] Y. A. Berlin, I. V. Kurnikov, D. Beratan, M. A. Ratner, and A. L. Burin, Top. Curr. Chem. **237**, 1 (2004).
[37] F. C. Grozema, L. D. A. Siebbeles, Y. A. Berlin, and M. A. Ratner, ChemPhysChem **3**, 536 (2002).
[38] K. Senthilkumar, F. C. Grozema, C. F. Guerra, F. M. Bickelhaupt, F. D. Lewis, Y. A. Berlin, M. A. Ratner, and L. D. A. Siebbeles, J. Am. Chem. Soc. **127**, 14894 (2005).
[39] Y. A. Berlin, A. L. Burin, and M. A. Ratner, Superlattices Microstruct. **28**, 241 (2000).
[40] Y. A. Berlin, A. L. Burin, and M. A. Ratner, J. Am. Chem. Soc. **123**, 260 (2001).

[41] A. Troisi and G. Orlandi, Chem. Phys. Lett. **344**, 509 (2001).
[42] T. Kubař, P. Benjamin Woiczikowski, G. Cuniberti, and M. Elstner, J. Phys. Chem. B **112**, 7937 (2008).
[43] T. Kubař and M. Elstner, J. Phys. Chem. B **112**, 8788 (2008).
[44] X. Xiao, B. Q. Xu, and N. J. Tao, Nano Lett. **4**, 267 (2004).
[45] S. Roche, Phys. Rev. Lett. **91**, 108101 (2003).
[46] S. Roche, D. Bicout, E. Macia, and E. Kats, Phys. Rev. Lett. **91**, 228101 (2003).
[47] E. M. Conwell and S. V. Rakhmanova, Proc. Natl. Acad. Sci. U.S.A. **97**, 4556 (2000).
[48] D. Hennig, Phys. Rev. E **64**, 041908 (2001).
[49] D. Hennig, E. B. Starikov, J. F. R. Archilla, and F. Palmero, J. Biol. Phys. **30**, 227 (2004).
[50] H. Yamada, Phys. Lett. A **332**, 65 (2004).
[51] R. Gutièrrez, S. Mohapatra, H. Cohen, D. Porath, and G. Cuniberti, Phys. Rev. B **74**, 235105 (2006).
[52] R. Gutierrez, S. Mandal, and G. Cuniberti, Nano Lett. **5**, 1093 (2005).
[53] R. Gutierrez, S. Mandal, and G. Cuniberti, Phys. Rev. B **71**, 235116 (2005).
[54] J. Yi, Phys. Rev. B **68**, 193103 (2003).
[55] G. Cuniberti, L. Craco, D. Porath, and C. Dekker, Phys. Rev. B **65**, 241314 (2002).
[56] H. Yamada, E. Starikov, and D. Hennig, Eur. Phys. J. B **59**, 185 (2007).
[57] D. Klotsa, R. A. Römer, and M. S. Turner, Biophys. J. **89**, 2187 (2005).
[58] E. Artacho, M. Machado, D. Sanchez-Portal, P. Ordejon, and J. M. Soler, Mol. Phys. **101**, 1587 (2003).
[59] P. J. DePablo, F. Moreno-Herrero, J. Colchero, J. GómezHerrero, P. Herrero, A. M. Baró, P. Ordejón, J. M. Soler, and E. Artacho, Phys. Rev. Lett. **85**, 4992 (2000).
[60] A. Hubsch, R. G. Endres, D. L. Cox, and R. R. P. Singh, Phys. Rev. Lett. **94**, 178102 (2005).
[61] Y. Zhang, R. H. Austin, J. Kraeft, E. C. Cox, and N. P. Ong, Phys. Rev. Lett. **89**, 198102 (2002).
[62] R. G. Endres, D. L. Cox, R. R. P. Singh, and S. K. Pati, Phys. Rev. Lett. **88**, 166601 (2002).
[63] J. P. Lewis, P. Ordejon, and O. F. Sankey, Phys. Rev. B **55**, 6880 (1997).
[64] A. Calzolari, R. DiFelice, E. Molinari, and A. Garbesi, J. Phys. Chem. B **108**, 2509 (2004).
[65] A. Calzolari, R. D. Felice, E. Molinari, and A. Garbesi, Appl. Phys. Lett. **80**, 3331 (2002).
[66] R. D. Felice, A. Calzolari, and E. Molinari, Phys. Rev. B **65**, 045104 (2001).
[67] R. D. Felice, A. Calzolari, and H. Zhang, Nanotechnology **15**, 1256 (2004).
[68] H. Zhang, A. Calzolari, and R. D. Felice, J. Phys. Chem. B **109**, 15345 (2005).
[69] F. L. Gervasio, A. Laio, M. Parrinello, and M. Boero, Phys. Rev. Lett. **94**, 158103 (2005).
[70] F. L. Gervasio, P. Carloni, and M. Parrinello, Phys. Rev. Lett. **89**, 108102 (2002).
[71] H. Mehrez and M. P. Anantram, Phys. Rev. B **71**, 115405 (2005).
[72] R. N. Barnett, C. L. Cleveland, A. Joy, U. Landman, and G. B. Schuster, Science **294**, 567 (2001).
[73] N. Rösch and A. A. Voityuk, Top. Curr. Chem. **237**, 37 (2004).
[74] A. A. Voityuk, J. Jortner, M. Bixon, and N. Rösch, Chem. Phys. Lett. **324**, 430 (2000).
[75] A. A. Voityuk, N. Rösch, M. Bixon, and J. Jortner, J. Phys. Chem. B **104**, 9740 (2000).
[76] A. Voityuk and N. Rösch, J. Phys. Chem. B **106**, 3013 (2002).
[77] A. A. Voityuk, J. Chem. Phys. **124**, 064505 (2006).
[78] D. N. Beratan, S. Priyadarshy, and S. M. Risser, Chem. Biol. **4**, 3 (1997).
[79] A. Sadowska-Aleksiejew, J. Rak, and A. A. Voityuk, Chem. Phys. Lett. **429**, 546 (2006).
[80] A. A. Voityuk, Chem. Phys. Lett. **439**, 162 (2007).
[81] A. A. Voityuk, K. Siriwong, and N. Rösch, Angew. Chem., Int. Ed. **43**, 624 (2004).
[82] F. C. Grozema, S. Tonzani, Y. A. Berlin, G. C. Schatz, L. D. A. Siebbeles, and M. A. Ratner, J. Am. Chem. Soc. **130**, 5157 (2008).
[83] M. A. O'Neill and J. K. Barton, Top. Curr. Chem. **236**, 67 (2004).
[84] M. A. O'Neill and J. K. Barton, J. Am. Chem. Soc. **126**, 11471 (2004).
[85] F. Shao, M. A. O'Neill, and J. K. Barton, Proc. Natl. Acad. Sci. U.S.A. **101**, 17914 (2004).
[86] M. A. O'Neill, H. Becker, C. Wan, J. K. Barton, and A. H. Zewail, Angew. Chem., Int. Ed. **42**, 5896 (2003).
[87] M. Elstner, D. Porezag, G. Jungnickel, J. Elsner, M. Haugk, T. Frauenheim, S. Suhai, and G. Seifert, Phys. Rev. B **58**, 7260 (1998).
[88] P.-O. Löwdin, J. Chem. Phys. **18**, 365 (1950).
[89] M. D. Newton, Chem. Rev. (Washington, D.C.) **91**, 767 (1991).
[90] V. Mujica, M. Kemp, and M. A. Ratner, J. Chem. Phys. **101**, 6849 (1994).
[91] V. Mujica, M. Kemp, and M. A. Ratner, J. Chem. Phys. **101**, 6856 (1994).
[92] J. Wang, P. Cieplak, and P. A. Kollman, J. Comput. Chem. **21**, 1049 (2000).
[93] A. Pérez, I. Marchán, D. Svozil, J. Šponer, T. E. Cheatham III, C. A. Laughton, and M. Orozco, Biophys. J. **92**, 3817 (2007).
[94] D. van der Spoel, E. Lindahl, B. Hess, G. Groenhof, A. E. Mark, and H. J. C. Berendsen, J. Comput. Chem. **26**, 1701 (2005).
[95] X. Lu and W. K. Olson, Nucleic Acids Res. **31**, 5108 (2003).
[96] http://structure.usc.edu/make-na/server.html.
[97] H. R. Drew, R. M. Wing, T. Takano, C. Broka, S. Tanaka, K. Itakura, and R. E. Dickerson, Proc. Natl. Acad. Sci. U.S.A. **78**, 2179 (1981).
[98] W. L. Jorgensen, J. Chandrasekhar, J. D. Madura, R. W. Impey, and M. L. Klein, J. Chem. Phys. **79**, 926 (1983).
[99] X. Lu, M. A. El Hassan, and C. A. Hunter, J. Mol. Biol. **273**, 681 (1997).
[100] C. R. Calladine and H. R. Drew, *Understanding DNA: The Molecule and How It Works* (Academic, New York, 1992).
[101] See EPAPS Document No. E-JCPSA6-130-004923 for further data analysis. For more information on EPAPS, see http://www.aip.org/pubservs/epaps.html.
[102] Y. A. Berlin, F. C. Grozema, L. D. A. Siebbeles, and M. A. Ratner, J. Phys. Chem. C **112**, 10988 (2008).
[103] A. Rodríguez, R. A. Römer, and M. S. Turner, Phys. Status Solidi B **243**, 373 (2006).
[104] S. Komineas, G. Kalosakas, and A. R. Bishop, Phys. Rev. E **65**, 061905 (2002).
[105] P. W. Anderson, Phys. Rev. **109**, 1492 (1958).
[106] I. A. Balabin, D. N. Beratan, and S. S. Skourtis, Phys. Rev. Lett. **101**, 158102 (2008).
[107] M. Büttiker and R. Landauer, Phys. Rev. Lett. **49**, 1739 (1982).
[108] U. Peskin, A. Edlund, I. Bar-On, M. Galperin, and A. Nitzan, J. Chem. Phys. **111**, 7558 (1999).
[109] A. Troisi, A. Nitzan, and M. A. Ratner, J. Chem. Phys. **119**, 5782 (2003).
[110] D. Reha, W. Barford, and S. Harris, Phys. Chem. Chem. Phys. **10**, 5436 (2008).
[111] G. B. Schuster, Acc. Chem. Res. **33**, 253 (2000).